

Measuring water retention in undisturbed samples of stony soils

Caroline Andrade Pereira¹, Rodrigo Pivoto Mulazzani¹, Quirijn de Jong Van Lier², Fabrício de Araújo Pedron¹, Paulo Ivonir Gubiani^{1*}

¹Universidade Federal de Santa Maria – Depto. de Solos, Av. Roraima, 1000 – 97105-900 – Santa Maria, RS – Brasil.

²Universidade de São Paulo/CENA – Lab. de Física do Solo, Av. Centenário, 303 – 13416-903 – Piracicaba, SP – Brasil.

*Corresponding author <paulo.gubiani@ufsm.br>

Edited by: Luiz Fernando Pires

Received July 27 2022

Accepted December 02, 2022

ABSTRACT: Stony soils have been increasingly used for agriculture production; however, little is known about their hydraulic properties due to problems, such as sample deformation and hydraulic continuity between samples and suction devices when the sampling and measurements are accomplished with traditional techniques. In this study, the traditional ring sampling technique was replaced by the sampling of undisturbed soil blocks coated with paraffin wax to preserve their structure. A saturated paste of fine-grained mineral particles was used to ensure contact and hydraulic continuity between samples and suction devices (sand table and ceramic plates). This allowed us to determine 30 water retention curves for three stony soils with coarse particle contents (> 2 mm) ranging from zero to 69 %. The van Genuchten model was fitted to the measured retention data and the root mean square errors were between 0.0034 and 0.0331 m³ m⁻³, with no outliers or odd behavior in the retention curves. These results showed that consistent water retention curves for stony soils can be determined with the technique proposed. Fine-grained minerals sandwiched between the surface of suctions sources and sampled blocks improve hydraulic continuity between them. These techniques can be applied to determine water retention properties in structured soil samples with coarse particles where it is unfeasible to collect structured soil samples with metal sampling rings.

Keywords: marginal soils, paraffined soil blocks, soil hydraulic properties

Introduction

The growing demand for food has driven soil occupation toward marginal soils around the world (European Commission, 2015). Research on these soils has increased worldwide in the last decades (Zhang et al., 2016); nevertheless, little is known about the hydraulic properties of stony soils (Zhang et al., 2016; Robertson et al., 2021) due to the difficulty of measuring them in samples from stony soils with rock (Novák et al., 2011).

The measurement of water retention properties in stony soils using conventional laboratory equipment, such as a sandbox (Stolte, 1997; Reinert and Reichert, 2006) or a pressure plate apparatus (Richards, 1965), is hindered by two main problems: (i) it is usually unfeasible to collect structured soil samples with rings in stony soils and (ii) it is challenging to ensure a good and continuous contact of soil samples containing stones to the porous media (ceramic plate, filter paper, or sand surface) used to apply tension and measure the water retention properties. Some measurements of water retention properties in stony soils sampled with metal rings are available (Al-Yahyai et al., 2006; Baetens et al., 2009; Khetdan et al., 2017; Ravina and Magier, 1984); however, these determinations are possibly biased due to unavoidable sample deformation during sampling when pushing the ring into the soil or because small cores may contain a representative volume of fragments and fine-earth. Even more bias may be expected in measurements of water retention properties performed in disturbed samples of stony soils (Grath et al., 2015; Gu et al., 2017). Thus, avoiding these challenges could contribute to improving knowledge of stony soil capability to hold and supply water to plants.

Undisturbed soil blocks sealed with paraffin wax or Saran resin is a technique used to preserve the soil structure, mainly in stony soils (Soil Survey Staff, 2014a). The hydraulic continuity between soil blocks and suction sources, such as sandboxes, tension tables or pressure chambers, could be accomplished with a moldable porous media with an air-entry value greater than that in the applied suction. To address these issues and improve techniques to determine the hydraulic properties in undisturbed samples of stony soil, we evaluated if the use of a paste of fine-grained sand and fine-grained quartz sandwiched between the suctions sources surface (sandbox and ceramic plate) and the surface of undisturbed soil blocks partially coated with paraffin wax enables the measurement of water retention properties for stony soils.

Materials and Methods

Soils

Soils with coarse fragments (CF), particles with apparent diameter between 2 and 200 mm, from three sites (identified as A, B and C) in southern Brazil were evaluated. The predominant soils are Typic Udorthent in site A (29°30'22" S, 53°37'34" W, 477 m) and Typic Dystrudept in sites B (30°14'2" S, 53°37'32" W, 271 m) and C (30°48'31" S, 53°30'41" W, 309 m), according to Soil Taxonomy (Soil Survey Staff, 2014b). These soils were formed from igneous rocks (rhyolite or rhyodacite in site A and granite in site B) and sedimentary (conglomerate in site C). Currently, soybean (*Glycine max* L.) and oat (*Avena strigosa* Schreb.) are cropped in sites A and B, while site C is covered by native grass.

Sampling and paraffin coating and bulk density determination

At the top of A horizon in each site, ten structured soil blocks were collected at several locations (between 100 to 200 m apart) to consider the variability of coarse fragments. Structured soil blocks were exposed by gently excavating up to 0.15 m of the surrounding soil with a knife, and shovel. After, the bottom part of the blocks was detached from the underlying soil with a knife and the blocks were wrapped with PVC food wrap and taken to the lab surrounded by wood saw-dust inside a box to minimize disturbance. At the same locations and depths, soil material (disturbed samples) was collected to determine the particle size distribution.

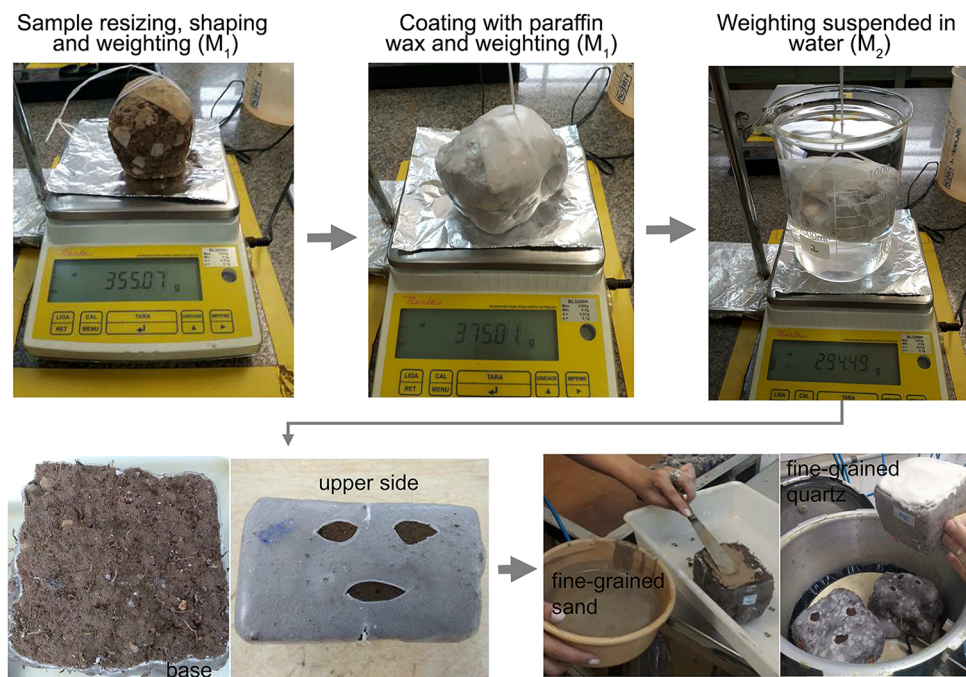
In the laboratory, the sampled soil blocks were gently resized and shaped with a small knife to approach their shape to a cube, which was more cumbersome in samples containing large fragments (Figure 1). In these samples, at least one *quasi*-flat surface was prepared as a sample base, necessary to ensure good contact with the porous medium used in tension or suction equipment, such as sandboxes and pressure chambers. The final size of samples was chosen (i) to avoid too large samples that would take a long time to reach potential water equilibrium in pressure chambers and (ii) to avoid too small samples, non-representative due to the exclusion of large coarse fragments. Sample volumes ranged from 354 to 1175 cm³; the largest samples had the biggest coarse fragments.

The main steps to determine the bulk density and water retention are shown in Figure 1. A thin plastic rope was tied around the soil blocks that were attached to a thin plastic rope and weighed (M_0). Subsequently, the blocks were immersed three times into melted paraffin wax (~ 60 °C) until complete coating (Blake, 1965; Soil Survey Staff, 2014a). The samples were again weighed after paraffin solidification (M_1). Then, the paraffin-coated samples were held suspended by the plastic rope and immersed in water inside a 1 L beaker, avoiding any contact with the walls or bottom of the beaker. The suspended weight (M_2) was registered to determine soil bulk density.

Based on the weights measured, the soil bulk density (ρ_b , kg m⁻³) of the soil blocks was calculated by using Archimedes' principle according to:

$$\rho_b = \frac{\frac{M_0}{W_g + 1}}{\frac{M_2}{\rho_a} - \frac{M_1 - M_0}{\rho_p}} \quad (1)$$

where: M_0 (kg) is the mass of the unsealed sample (without paraffin), W_g (kg kg⁻¹) is the mass-based water content of the sample (see Eq. (6) below), M_1 (kg) is the mass of the sealed sample (including paraffin); M_2 (kg) is the displaced mass of water by the paraffined sample held suspended in water (Figure 1); ρ_a (1000 kg m⁻³) and ρ_p (900 kg m⁻³) are water and paraffin densities, respectively.



Sample base and upper opening, and base covering with saturated fine-grained sand and saturated fine-grained quartz for water retention measurements in sand table and pressure plate.

Figure 1 – Main steps used to determine bulk density and water retention.

Water retention

As the sample should allow water inflow (for saturation) and outflow (drainage on sand table and ceramic plate), the paraffin covering the sample base was removed and three small holes were opened in the paraffin at the upper side of the sample (Figure 1). Samples were "saturated" (the achievable degree of saturation with this procedure) upside down in a tray with water to reduce air entrapment and soil material loss from the sample base. The water level was slowly raised to promote saturation, mainly by a capillary rise. After 48 h, the sample mass (M_s) was recorded to determine its effective saturation.

A paste of fine-grained sand was applied to the sample base to ensure hydraulic continuity between the sample and the sandbox surface. This fine-grained sand had 7 % of coarse and very coarse sand (2.0-0.5 mm), 50 % of medium sand (0.5-0.25 mm), 39 % of fine sand (0.25-0.10 mm), 3 % of very fine sand (0.10-0.05 mm) and 1 % of silt (< 0.05 mm). The paste of saturated fine-grained sand of approximately 0.5 cm height firmly attached the sample to the sandbox surface improving the hydraulic continuity between them (Figure 1). A piece of cloth screen was used between the sample sand layer and the sandbox surface to minimize the attachment of sand to the samples when removing them from the sandbox. Water suction in the sandbox was increased from zero (initially saturated) to 0.6 m (a typical suction to distinguish macro and micropores). It was kept at this value for 48 h (Gubiani et al., 2009). After that, the mass of the samples with sand layer was recorded ($M_{0.6}$), the samples were re-saturated as previously described (upside down), and returned to the sandbox. Water suction in the sandbox was increased to 1.0 m (a typical suction used to estimate field capacity) and kept at this value for 72 h after which the mass of samples with sand layer was recorded ($M_{1.0}$).

The fine-grained sand layer on the sample base was removed and weighed (M_{FS}). Samples were then prepared to be submitted to the pressure apparatus. After resaturation (upside down), fine-grained quartz was used to ensure hydraulic continuity between the sample and ceramic plate in the pressure apparatus (Figure 1). This fine-grained quartz contained 2 % of coarse and very coarse sand (2.0-0.5 mm), 1 % of medium sand (0.5-0.25 mm), 39 % of fine sand (0.25-0.10 mm), 32 % of very fine sand (0.10-0.05 mm) and 26 % of silt (< 0.05 mm). The air-entry value of the fine-grained quartz is not known, but tests showed that its water potential (measured with Teros 21 by Meter Inc) decreased to the corresponding pressure applied in the pressure chamber. Samples were placed on the porous plate and a 10 m pressure head was applied. The mass of the samples with fine-grained quartz (M_{10}) was determined after 30 to 40 d of pressure, when water outflow was no longer detected. Next, the fine-grained quartz on the sample base was removed and weighed (M_Q). All remaining paraffin was also

removed and weighed (M_P) and the sample was oven dried at 105 °C for 48 h and then weighed again (M_D). In all steps, samples were carefully handled to avoid the loss of their components (M_{FS} , M_Q , M_P , and M_D). Soil particles that remained attached on the paraffin after its detachment from the soil sample, the fine-grained sand and the fine-grained quartz particles attached to the sample base, were all carefully removed with a soft brush and weighted together with the respective component.

Volumetric water content at effective saturation (θ_s) and the suctions of 0.6 m ($\theta_{0.6}$), 1.0 m ($\theta_{1.0}$), and 10 m (θ_{10}) was calculated as:

$$\theta_s = \frac{(M_s - M_P - M_D) \rho_b}{M_D \rho_a} \quad (2)$$

$$\theta_{0.6} = \frac{(M_{0.6} - M_{FS} - M_P - M_D) \rho_b}{M_D \rho_a} \quad (3)$$

$$\theta_{1.0} = \frac{(M_{1.0} - M_{FS} - M_P - M_D) \rho_b}{M_D \rho_a} \quad (4)$$

$$\theta_{10} = \frac{(M_{10} - M_Q - M_P - M_D) \rho_b}{M_D \rho_a} \quad (5)$$

where: M_s , $M_{0.6}$, $M_{1.0}$, M_{10} , M_{FS} , M_Q , M_P , M_D (kg), ρ_b (kg m⁻³) and ρ_a (= 1000 kg m⁻³) were all previously described.

The mass-based water content W_g needed for ρ_b determination (Eq. (1)) was then calculated as:

$$W_g = \frac{M_0 - M_D}{M_D} \quad (6)$$

Water retention at suctions higher than 100 m was determined with a dewpoint water potential meter, model WP4C (Decagon Devices, 2007). The WP4C measures water potential from 0 to -1000 m with an accuracy of -10 m and from -1000 to -30000 m with an accuracy of 1 %. Measurements were performed as proposed by Gubiani et al. (2021b) for coarse soils. For that purpose, all dried soil blocks were gently disturbed to avoid the breakdown of coarse material. About 100 g of this disturbed sample (DS) was sieved through a 4-mm mesh. For soils with particles with apparent diameters greater than 4 mm (sites A and C), the particles were fractured to sizes smaller than 4 mm and then mixed with the non-fractured particles smaller than 4 mm. The mixed material was moistened and kept hermetically sealed in the laboratory room for 24 h to allow water redistribution (Campbell et al., 2007). Afterward, the water-potential relation in the range -100 to -1000 m (four to seven measurements) was determined as described in Gubiani et al. (2013), converting mass- to volume base by multiplying by ρ_b/ρ_a .

The van Genuchten (1980) function [Eq. (7)] was fitted to the data of each sample individually (θ_s , $\theta_{0.6}$, $\theta_{1.0}$, θ_{10} , and WP4C data) by minimizing the squared sum of residuals with the PROC NLIN of the Statistical Analysis System software (SAS Institute, 1999).

$$\theta = \theta_r + (\theta_s - \theta_r) [1 + (\alpha h)^n]^{-1} \quad (7)$$

in Eq. (7), h (m) is the suction or absolute value of the matric potential, θ , θ_s , and θ_r ($\text{m}^3 \text{m}^{-3}$) are the estimated, saturated, and residual water content, respectively, α (m^{-1}), and n (dimensionless) are fitting parameters. θ_r was also constrained to non-negative values ($\theta_r \geq 0$).

Particle size distribution

Disturbed samples were used to determine the particle size distribution, separating between cobbles and coarse gravel (CCG, 250 – 20 mm), medium and fine gravel (MFG, 20 – 2 mm), coarse sand (CS, 2 – 0.25 mm), fine sand (FS, 0.25 – 0.05 mm), silt (0.05 – 0.002 mm) and clay (< 0.002 mm) (Schoeneberger et al., 2012). Sand, silt, and clay were determined by shaking 20 g of the soil fraction passed in a 2 mm mesh sieve in a solution of 1 mol L⁻¹ NaOH with a horizontal reciprocating shaking during (i) 4 h and with nylon spheres for soils of site B and C (not containing fragile sand particles) (Suzuki et al., 2015) and (ii) 2 h and without nylon spheres for soil A, due to the presence of fragile sand particles (Gubiani et al., 2021a). The sand fraction was separated by washing the dispersed sample on a 0.053 mm mesh sieve and the clay fraction was determined with the pipette method (Gee and Or, 2002), while silt was calculated as the remaining part after subtracting sand and clay from the whole sample mass. To determine CCG and MFG fractions, particles retained in the 2 mm mesh sieve were immersed in a solution of 1 M NaOH and gently stirred for 15 min. Next, the particles were washed with water, dried at 105 °C for 48 h, sieved (20 mm-mesh), and weighed.

Data analysis

A cumulative mean particle size distribution curve and its standard deviation were used to show the particle size distribution over the classes CCG, MFG, CS, FS, silt and clay. The goodness of fit of Eq. (7) was evaluated considering the root mean of squared errors (RMSE) and the curve shapes were evaluated graphically.

Results

The fraction of particles within the six particle size classes varied considerably among the samples of the three soils (Figure 2). In all samples from site B, two from sites A, and seven from site C, there were no cobbles and coarse gravel particles (GCC, 250 – 20 mm). Medium and fine gravel particles (MFG, 20 – 2 mm) were absent in two samples from sites A. However, the fraction of particles larger than coarse sand (CCG + MFG) ranged from 20 to 53 % at site A, 6 to 40 % at site B, and 7 to 48 % at site C. A greater amount of coarse sand occurred in sites B (28 to 48 %) and C (14 to 47 %), while site A showed a

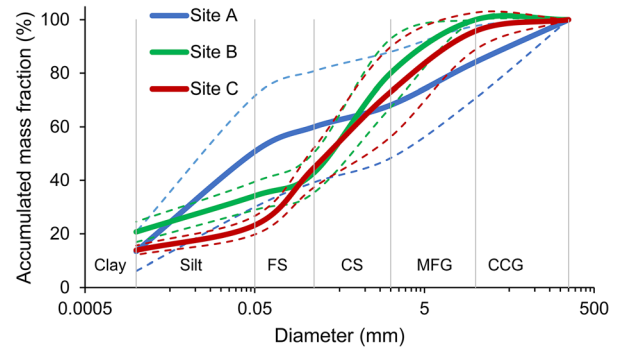


Figure 2 – Particle size distribution curves for sites A, B, and C. FS = fine sand; CS = coarse sand; MFG = medium and fine gravel; CCG = cobbles and coarse gravel. Solid lines correspond to mean values, and dotted lines represent the mean \pm SD values. Vertical lines represent the limit of particles classes.

greater presence of silt (24 to 63 %). The amount of clay did not exceed 26 % in sites A and B and 17 % in site C. Bulk density was around 1.20 g cm⁻³ (\pm 0.07) in site A and around 1.60 (\pm 0.05) g cm⁻³ in sites B and C.

The van Genuchten model fitted well to the retention data, with RMSE ranging from 0.0034 (site C) to 0.0331 m³ m⁻³ (site A) and R² ranging from 0.96 to 0.99 (Table 1). In this range, 80 and 60 % of the RMSE values were below 0.010 m³ m⁻³ in sites B and C, respectively. In site A, all RMSEs were greater than 0.010 m³ m⁻³ and 80 % were between 0.020 and 0.0331 m³ m⁻³. The values of θ_s ranged from 0.325 m³ m⁻³ (site B) to 0.585 m³ m⁻³ (site A), with a negative correlation (Pearson) with bulk density (-0.99 , $p < 0.001$). The large θ_s in site A was attributed to its porous rock fragments (around 0.4 m³ m⁻³ of total porosity - data not shown). In only three cases, θ_r was different (slightly greater) than zero. There was great variability in parameter α (0.263 to 48.240 m⁻¹), with values increasing from site A to C to B. Parameter n varied between 1.115 and 1.601.

Typical “S” - shaped curves were obtained for the three soils (Figure 3). The decrease in measured θ (h) at the transitions between equipment ($h = 1$ m in the sand column to $h = 10$ m in the pressure chamber, and then to $h > 50$ m in WP4) does not indicate any inconsistency even in the curves with low-quality fits (red line). The small variability of n and θ_r (Table 1) among the samples of each soil is reflected in the approximation of the final segment of the curves for values of θ around 0.010 m³ m⁻³ in h of 1000 m (Figure 2), while higher α values in B and C (Table 1) implied a more pronounced reduction of θ at the start of the retention curve.

Discussion

Determining the water retention curve using data from tension tables and pressure plate apparatus unavoidably contains uncertainty, regardless of the type of sample used. On the one hand, it is possible

Table 1 – van Genuchten model parameters (Eq. 7) for each sample of sites A, B, and C.

Sample	θ_s	θ_r	α	n (-)	RMSE	R ²
	m ³ m ⁻³					
Site A						
1	0.550	0.000	0.382	1.338	0.0281	0.97
2	0.536	0.000	0.599	1.287	0.0274	0.97
3	0.544	0.000	0.495	1.311	0.0218	0.98
4	0.529	0.000	0.557	1.284	0.0208	0.98
5	0.494	0.000	0.263	1.347	0.0125	0.99
6	0.585	0.000	1.240	1.279	0.0331	0.96
7	0.556	0.000	0.885	1.267	0.0226	0.98
8	0.584	0.000	0.666	1.282	0.0290	0.96
9	0.471	0.000	0.363	1.297	0.0239	0.97
10	0.493	0.000	0.264	1.316	0.0175	0.98
Site B						
1	0.355	0.000	11.083	1.126	0.0088	0.98
2	0.325	0.071	15.387	1.181	0.0041	0.99
3	0.363	0.000	14.068	1.143	0.0054	0.99
4	0.345	0.000	14.044	1.115	0.0050	0.99
5	0.356	0.000	11.037	1.127	0.0061	0.99
6	0.346	0.000	48.240	1.136	0.0063	0.98
7	0.349	0.000	22.995	1.152	0.0078	0.98
8	0.367	0.000	11.836	1.136	0.0107	0.97
9	0.364	0.000	7.004	1.167	0.0108	0.97
10	0.327	0.000	3.397	1.154	0.0070	0.99
Site C						
1	0.348	0.000	8.052	1.244	0.0046	0.99
2	0.377	0.000	7.868	1.233	0.0129	0.97
3	0.354	0.000	5.785	1.233	0.0111	0.98
4	0.367	0.000	18.248	1.214	0.0041	0.99
5	0.363	0.000	5.700	1.229	0.0058	0.98
6	0.342	0.000	5.447	1.210	0.0034	0.99
7	0.344	0.000	8.962	1.188	0.0054	0.99
8	0.365	0.000	5.123	1.206	0.0113	0.98
9	0.351	0.024	8.802	1.243	0.0032	0.99
10	0.390	0.071	2.524	1.601	0.0151	0.96

θ_s , and θ_r (m³ m⁻³) are the saturated and residual water content, respectively, α (m⁻¹), and n (dimensionless) are fitting parameters; RMSE (m³ m⁻³) = the root mean square error; R² = the coefficient of determination.

to precisely define the water tension in the porous medium of the equipment. However, ensuring a hydraulic continuum or potential water equilibrium between the sample and the equipment is impossible. The hydraulic continuum cannot be directly observed during measurements and indirect confirmation via measurement of the sample water matric potential by tensiometers is complex and hardly ever performed. Drilling regular holes in the samples to insert tensiometers in soils with rock fragments is even more challenging. Therefore, the *h* value in the sample at the end of equilibration on the tension table or pressure plate apparatus is uncertain. This shows that several aspects related to curve fitting need to be considered. Thus, retention curves obtained in this study will be evaluated and discussed.

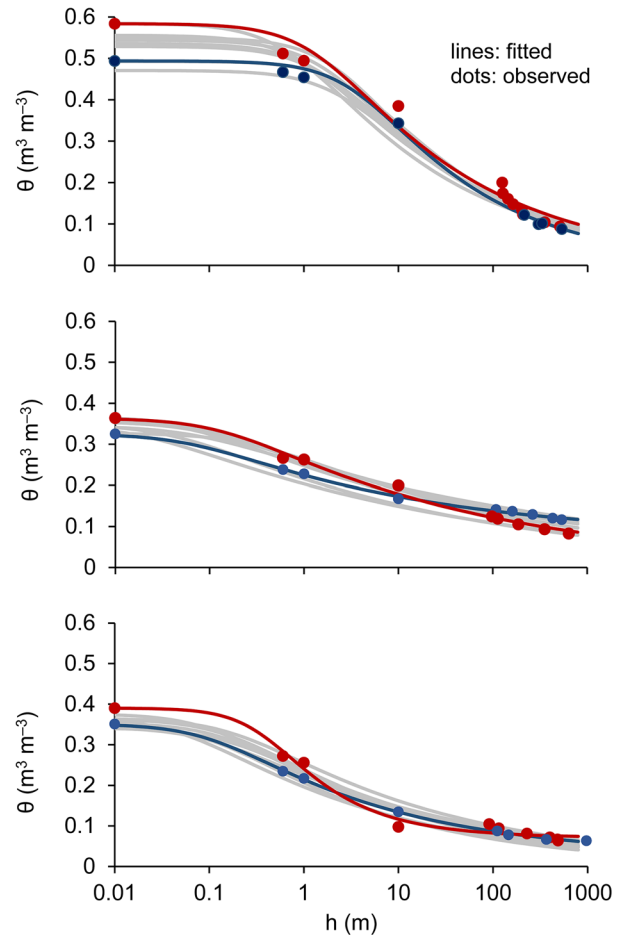


Figure 3 – Soil water retention curves for all samples of sites A, B, and C. The red and blue lines are the worst and best fit of van Genuchten model (Eq. 7), and the red and blue dots are their respective observed data used for fitting.

Incomplete water potential equilibrium, that is, incomplete water extraction at each tension does not necessarily result in visible deviations in the shape of the retention curve. On the other hand, the fact that no apparent deviation of data points is observed concerning the fitted curve does not mean that observations correspond to a perfect equilibrium. The θ (*h*) curves described by the van Genuchten equation (Eq. (7)) were very close to the θ measurements, even in the samples with the worst fit (Figure 3) and the maximum RMSE was 0.0331 m³ m⁻³ (Table 1). The RMSE range for the soils in our study is similar to observations of fitting the van Genuchten equation in soils of different textural classes with (Grath et al., 2015) and without rock fragments (Baetens et al., 2009; Armindo et al., 2019).

Nonetheless, good correspondence between fitted and measured curves, expressed by a low RMSE, may occur if a segment or the entire curve is affected by incomplete extraction of water over adjacent data points. The samples in our study showed no clear

evidence that this may have occurred (Figure 3). The relationship $\theta(h)$ determined with WP4 ($h > 50$ m in Figure 3) is obtained by measuring both θ and h . Therefore, the segment $\theta(h)$ determined by WP4 does not suffer from equilibrium issues and may be considered more reliable (Gubiani et al., 2013; De Jong van Lier et al., 2019), carrying less uncertainty than the segment obtained in the sandbox and pressure plate apparatus. If the segment obtained in a sandbox and pressure plate apparatus decreases gradually and coherently converges to the more reliable segment determined by WP4 then the uncertainty for the sandbox and pressure plate apparatus may also be considered low. In the samples used in this study, all curves show a gradual and coherent change of θ between $h_{0.6m}$ and h_{1m} and between h_{10m} and h_{100m} (Figure 3).

There is also no evidence of incomplete equilibrium when comparing the decrease in θ of the samples in our study with the decrease in θ reported in the literature for the same h intervals. For example, between $h = 0$ and 0.6 m and between 1 and 10 m, θ decreased by an average of $0.09 \text{ m}^3 \text{ m}^{-3}$ and $0.07 \text{ m}^3 \text{ m}^{-3}$, respectively. This decrease is slightly smaller than the average decrease of θ ($0.13 \text{ m}^3 \text{ m}^{-3}$ and $0.08 \text{ m}^3 \text{ m}^{-3}$) in the same h intervals above for the CRA of 13 soil textural classes from the model database Hydrus-1D (Simunek et al., 2005).

Another important aspect is that incomplete equilibrium is more common at very high pressures, such as $h = 150$ m (De Jong van Lier et al., 2019). In our study, the highest h applied was 10 m. Therefore, the evidence analyzed indicates that the fine-grained sand and fine-grained quartz applied to the sample base promoted enough continuity between the sample and the porous media of the sandbox and pressure plate apparatus, respectively. This strategy combined with waterproofing of soil blocks with paraffin wax allowed to determine coherent water retention curves for undisturbed samples of stony soils, which contribute to a better knowledge of their hydraulic properties. However, this strategy may fail for soils with cohesion insufficient to keep a structured soil block, such as soils with high stone and sand contents. For these cases, a modified method may be needed.

Conclusions

Consistent water retention curves for stony soils can be determined with undisturbed soil blocks partially coated with paraffin wax. Using a paste of fine-grained sand and fine-grained quartz sandwiched between the surface of suction sources (sandbox and ceramic plate) and the surface of sampled blocks ensured hydraulic continuity between them at first glance. These techniques can be applied elsewhere to determine water retention properties in structured soil samples with coarse particles where it is unfeasible to collect structured soil samples with rings.

Acknowledgments

This research was funded by the Coordenação de Aperfeiçoamento de Pessoal de Nível Superior (CAPES) – Código de Financiamento 001, and the Conselho Nacional de Desenvolvimento Científico e Tecnológico (CNPq) - Processo 434853/2018-6.

Authors' Contributions

Conceptualization: Gubiani, P.I.; Pereira, C.A.; De Jong Van Lier, Q. **Formal analysis:** Gubiani, P.I.; Pereira, C.A. **Investigation:** Pereira, C.A. **Methodology:** Pereira, C.A.; Gubiani, P.I. **Supervision:** Gubiani, P.I. **Writing – original draft:** Pereira, C.A.; Gubiani, P.I. **Writing – review & editing:** Gubiani, P.I.; Pereira, C.A.; De Jong Van Lier, Q.; Mulazzani, R.P.; Pedron, F.A.

References

- Al-Yahyai, R.; Schaffer, B.; Davies, F.S.; Muñoz-Carpena, R. 2006. Characterization of soil-water retention of a very gravelly loam soil varied with determination method. *Soil Science* 171: 85-93. <https://doi.org/10.1097/01.ss.0000187372.53896.9d>
- Armindo, R.A.; De Jong van Lier, Q.; Turek, M.E.; Reis, A.M.H.; Melo, M.L.A.; Ramos, M.E.P.; Ono, G.M. 2019. Performance of the groenevelt and grant model for fitting soil water retention data from brazilian soils. *Revista Brasileira de Ciência do Solo* 43: 1-12. <https://doi.org/10.1590/18069657rbcs20180217>
- Baetens, J.M.; Verbist, K.; Cornelis, W.M.; Gabriels, D.; Soto, G. 2009. On the influence of coarse fragments on soil water retention. *Water Resources Research* 45: 1-14. <https://doi.org/10.1029/2008WR007402>
- Blake, G.R. 1965. Bulk density. p. 374-390. In: Black, C.A., ed. *Methods of soil analysis. Part 1. Physical and mineralogical properties, including statistics of measurement and sampling.* Soil Science Society of America, Madison, WI, USA. (Agronomy Monograph). <https://doi.org/10.2134/agronmonogr9.1.c30>
- Campbell, G.S.; Smith, D.M.; Teare, B.L. 2007. Application of a dew point method to obtain the soil water characteristic. p. 71-77. In: Schanz, T., ed. *Experimental unsaturated Pullman, WA, USA. soil mechanics.* Springer, Berlin, Germany. https://doi.org/https://doi.org/10.1007/3-540-69873-6_7
- Decagon Devices. 2007. WP4 Dewpoint Potentiometer: Operator's Manual. 5ed. Decagon Devices.
- De Jong Van Lier, Q.; Pinheiro, E.A.R.; Inforsato, L. 2019. Hydrostatic equilibrium between soil samples and pressure plates used in soil water retention determination: consequences of a questionable assumption. *Revista Brasileira de Ciência do Solo* 43: 1-14. <https://doi.org/10.1590/18069657rbcs20190014>
- European Commission. Institute for Environment and Sustainability. 2015. *Soil Atlas of Latin America and the Caribbean.* European Commission, Brussels, Belgium. <https://data.europa.eu/doi/10.2788/912516>
- Gee, G.W.; Or, D. 2002. 2.4 Particle-size analysis. p. 255-293. In: Dane, J.H.; Topp, G.C., eds. *Methods of soil analysis. Part 4. Physical methods.* Soil Science Society of America, Madison, WI, USA. <https://doi.org/10.2136/sssabookser5.4.c12>

- Grath, S.M.; Ratej, J.; Jovičić, V.; Curk, B.C. 2015. Hydraulic characteristics of alluvial gravels for different particle sizes and pressure heads. *Vadose Zone Journal* 14: 1-18. <https://doi.org/10.2136/vzj2014.08.0112>
- Gu, F.; Ren, T.; Li, B.; Li, L. 2017. Accounting for calcareous concretions in calcic vertisols improves the accuracy of soil hydraulic property estimations. *Soil Science Society of America Journal* 81: 1296-1302. <https://doi.org/10.2136/sssaj2017.02.0046>
- Gubiani, P.I.; Albuquerque, J.A.; Reinert, D.J.; Reichert, J.M. 2009. Water tension and extraction by suction table and sand suction column in two soils with high bulk density. *Ciencia Rural* 39: 2535-2538 (in Portuguese, with abstract in English). <https://doi.org/10.1590/S0103-84782009005000199>
- Gubiani, P.I.; Reichert, J.M.; Campbell, C.; Reinert, D.J.; Gelain, N.S. 2013. Assessing errors and accuracy in dew-point potentiometer and pressure plate extractor measurements. *Soil Science Society of America Journal* 77: 19-24. <https://doi.org/10.2136/sssaj2012.0024>
- Gubiani, P.I.; Almeida, T.A.; Mulazzani, R.P.; Pedron, F.A.; Suzuki, L.E.A.S.; Pereira, C.A. 2021a. Shaking settings to reduce the breakdown of Entisol fragile particles in texture analysis. *Revista Brasileira de Ciência do Solo* 45: 1-14. <https://doi.org/10.36783/18069657rbcs20210066>
- Gubiani, P.I.; Pereira, C.A.; Cauduro, J.S.; Campbell, C.; Rivera, L.; Pigatto, C.S.; França, J.S. 2021b. Rock size fragments reduction allow including their effect on water retention properties determined with a dew point potentiometer. *Revista Brasileira de Ciência do Solo* 45: 1-11. <https://doi.org/10.36783/18069657rbcs20200182>
- Khetdan, C.; Chittamart, N.; Tawornpruek, S.; Kongkaew, T.; Onsamrarn, W.; Garré, S. 2017. Influence of rock fragments on hydraulic properties of Ultisols in Ratchaburi Province, Thailand. *Geoderma Regional* 10: 21-28. <https://doi.org/10.1016/j.geodrs.2017.04.001>
- Novák, V.; Kňava, K.; Šimůnek, J. 2011. Determining the influence of stones on hydraulic conductivity of saturated soils using numerical method. *Geoderma* 161: 177-181. <https://doi.org/10.1016/j.geoderma.2010.12.016>
- Ravina, I.; Magier, J. 1984. Hydraulic conductivity and water retention of clay soils containing coarse fragments. *Soil Science Society of America Journal* 48: 736-740. <https://doi.org/10.2136/sssaj1984.03615995004800040008x>
- Reinert, D.J.; Reichert, J.M. 2006. Use of sand column to measure soil water retention: prototypes and test. *Ciencia Rural* 36: 1931-1935 (in Portuguese, with abstract in English). <https://doi.org/10.1590/s0103-84782006000600044>
- Richards, L. 1965. Physical conditions of water in soil. p. 128-152. In: Black, C.; Evans, D.D.; White, J.L.; Clark, F.E., eds. *Methods of soil analysis: physical and mineralogical properties, including statistics of measurements and sampling*. Soil Science Society of America, Madison, WI, USA.
- Robertson, B.B.; Almond, P.C.; Carrick, S.T.; Penny, V.; Chau, H.W.; Smith, C.M.S. 2021. Variation in matric potential at field capacity in stony soils of fluvial and alluvial fans. *Geoderma* 392: 114978. <https://doi.org/10.1016/j.geoderma.2021.114978>
- Schoeneberger, P.J.; Wysocki, D.A.; Benham, E.C. 2012. *Field book for describing and sampling soils, version 3.0*. USDA-NRCS, Washington, DC, USA. <https://www.nrcs.usda.gov/sites/default/files/2022-09/field-book.pdf>
- Šimůnek, J.; van Genuchten, M.T.; Šejna, M. 2005. *The HYDRUS-1D Software Package for Simulating the One-Dimensional Movement of Water, Heat and Multiple Solutes in Variably-Saturated Media, Version 3.0*. California University Department of Environmental Sciences, Riverside, CA, USA.
- Soil Survey Staff. 2014a. *Kellogg Soil Survey Laboratory Methods Manual: Version 5.0*. R. USDA-NRCS, Washington, DC, USA. (Soil Survey Investigations Report, 42).
- Soil Survey Staff. 2014b. *Keys to Soil Taxonomy*. 12ed. USDA-NRCS, Washington, DC, USA.
- Stolte, J. 1997. *Manual For Soil Physical Measurements: Version 3*. DLO-Staring Centre, Wageningen, The Netherlands. (Technical Document, 37) <https://edepot.wur.nl/356797>
- Suzuki, L.E.A.S.; Reichert, J.M.; Albuquerque, J.A.; Reinert, D.J.; Kaiser, D.R. 2015. Dispersion and flocculation of Vertisols, Alfisols and Oxisols in southern Brazil. *Geoderma Regional* 5: 64-70. <https://doi.org/10.1016/j.geodrs.2015.03.005>
- van Genuchten, M.T. 1980. A closed-form equation for predicting the hydraulic conductivity of unsaturated soils. *Soil Science Society of America Journal* 44: 892-898. <https://doi.org/10.2136/sssaj1980.03615995004400050002x>
- Zhang, Y.; Zhang, M.; Niu, J.; Li, H.; Xiao, R.; Zheng, H.; Bech, J. 2016. Rock fragments and soil hydrological processes: significance and progress. *Catena* 147: 153-166. <https://doi.org/10.1016/j.catena.2016.07.012>